iScience

CellPress
OPEN ACCESS

Article

Mitochondrial CMPK2 mediates immunomodulatory and antiviral activities through IFN-dependent and IFN-independent pathways

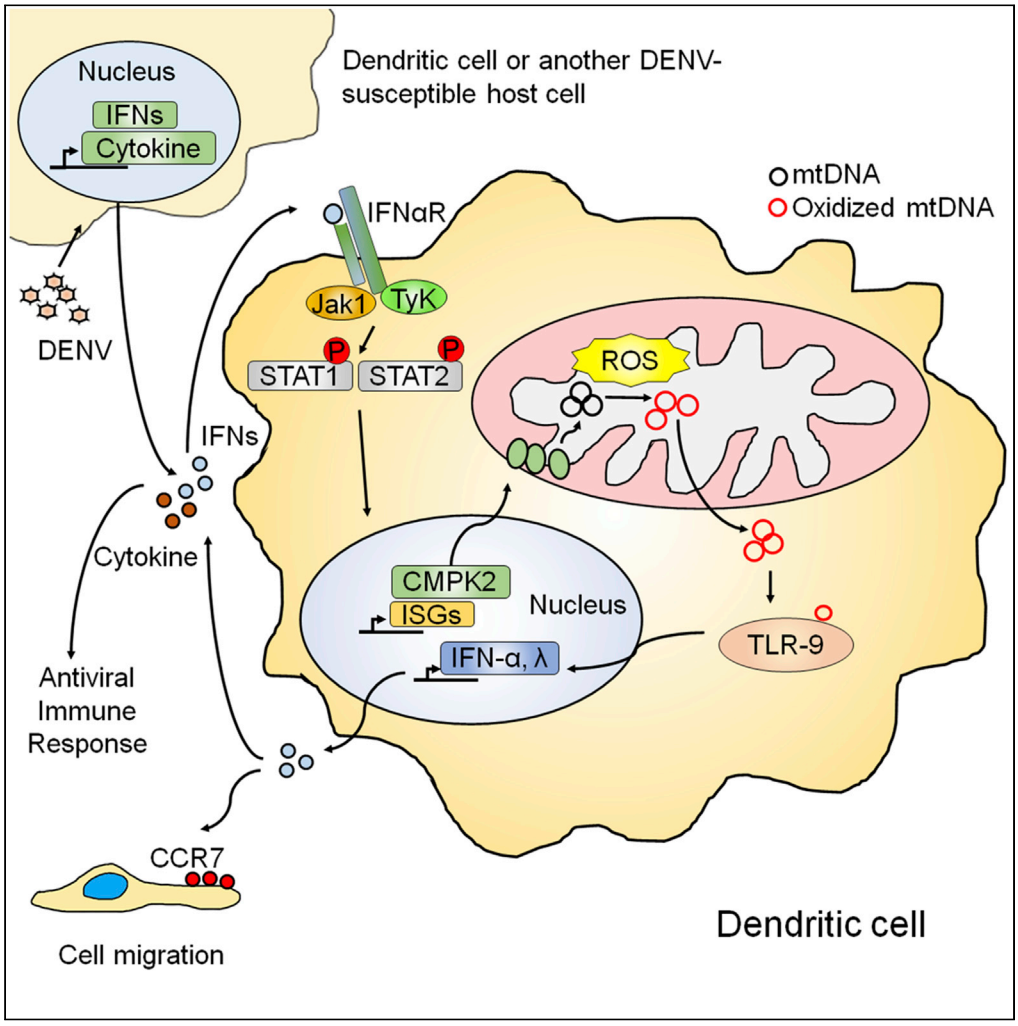

Jenn-Haung Lai, De-Wei Wu, Chien-Hsiang Wu, ..., Ann Chen, Zee-Fen Chang, Ling-Jun Ho

lingjunho@nhri.org.tw

Highlights

DENV infection induces mitochondrial CMPK2 that suppresses viral replication

CMPK2 is involved in DENV-induced IFNs but not TNF-α production

CMPK2-KO attenuates DENV-induced mtDNA release into cytosol and mtROS production

CMPK2 mediates antiviral activities via IFN-dependent and IFN-independent pathways

Lai et al., iScience 24, 102498
June 25, 2021 © 2021
https://doi.org/10.1016/j.isci.2021.102498

iScience

CellPress
OPEN ACCESS

Article

Mitochondrial CMPK2 mediates immunomodulatory and antiviral activities through IFN-dependent and IFN-independent pathways

Jenn-Haung Lai,[1] De-Wei Wu,[1] Chien-Hsiang Wu,[1] Li-Feng Hung,[2] Chuan-Yueh Huang,[2] Shuk-Man Ka,[3] Ann Chen,[4] Zee-Fen Chang,[5] and Ling-Jun Ho[2,6,*]

SUMMARY

Mitochondria regulate the immune response after dengue virus (DENV) infection. Microarray analysis of genes identified the upregulation of mitochondrial cytidine/uridine monophosphate kinase 2 (CMPK2) by DENV infection. We used small interfering RNA-mediated knockdown (KD) and CRISPR-Cas9 knockout (KO) approaches, to investigate the role of CMPK2 in mouse and human cells. The results showed that CMPK2 was critical in DENV-induced antiviral cytokine release and mitochondrial oxidative stress and mitochondrial DNA release to the cytosol. The DENV-induced activation of Toll-like receptor (TLR)-9, inflammasome pathway, and cell migration was suppressed by CMPK2 depletion; however, viral production increased under CMPK2 deficiency. Examining mouse bone marrow-derived dendritic cells from interferon-alpha (IFN-α) receptor-KO mice and signal transducer and activator of transcription 1 (STAT1)-KO mice, we confirmed that CMPK2-mediated antiviral activity occurred in IFN-dependent and IFN-independent manners. In sum, CMPK2 is a critical factor in DENV-induced immune responses to determine innate immunity.

INTRODUCTION

Dengue virus (DENV) infection is a critical public health issue worldwide (Castro et al., 2017). Infection with DENV can lead to catastrophic manifestations such as dengue hemorrhagic fever (DHF) and dengue shock syndrome (DSS). Although many comorbid conditions may be influential (Whitehorn and Simmons, 2011), the production and release of proinflammatory cytokines into the blood resulting in an overwhelming immune response has been recognized as the major cause of life-threatening presentations in patients with DENV infection (Paessler and Walker, 2013). In addition, the release of antiviral cytokines, such as type I and type III interferons (IFNs) is another hallmark of DENV infection (Ngono and Shresta, 2018). The complex mechanisms of DENV infection-mediated immunopathogenesis make the treatment of lethal DENV infection a great challenge, and thus far, no promising medications are available for successfully treating this disease (Lai et al., 2017).

Among the organelles in virus-infected cells, the mitochondria function as the pivotal organelle in triggering antiviral immunity and, at times, may also be targeted by viruses to evade immune surveillance (Chatel-Chaix et al., 2016). Several recognizable events, such as the generation of reactive oxygen species (ROS) in the mitochondria (mtROS), the release of mitochondrial DNA (mtDNA), and the induction of mitophagy, can lead to the activation of the inflammasome pathway and inflammatory response (van der Burgh and Boes, 2015). Many critical immune effector cells, such as dendritic cells (DCs), macrophages, T lymphocytes, and B lymphocytes, have close interactions with metabolic signaling pathways (Pearce and Pearce, 2013). IFNs can also regulate mitochondrial function by affecting cellular metabolism, fatty acid oxidation, and oxidative phosphorylation (Wu et al., 2016). Our previous report demonstrated that circular mtDNA containing nonmethylated CpG motifs is an important mediator driving proinflammatory reactions in DENV infection (Lai et al., 2018).

To identify candidate mitochondrial molecules critical for immune responses triggered by DENV infection, microarray analysis was carried out in human DCs that were mock infected or infected with DENV. Among the many upregulated and downregulated genes, the cytidine/uridine monophosphate kinase 2 (CMPK2)

[1]Department of Rheumatology, Allergy and Immunology, Chang Gung Memorial Hospital, Lin-Kou, Tao-Yuan, Taiwan, R.O.C

[2]Institute of Cellular and System Medicine, National Health Research Institute, Zhunan, Taiwan, R.O.C

[3]Graduate Institute of Aerospace and Undersea Medicine, Department of Medicine, National Defense Medical Center, Taipei, Taiwan, ROC

[4]Department of Pathology, Tri-Service General Hospital, National Defense Medical Center, Taipei, Taiwan

[5]Institute of Molecular Medicine, College of Medicine, National Taiwan University, Taipei 10002, Taiwan

[6]Lead contact

*Correspondence: lingjunho@nhri.org.tw

https://doi.org/10.1016/j.isci.2021.102498

This is an open access article under the CC BY-NC-ND license (http://creativecommons.org/licenses/by-nc-nd/4.0/).

gene (also known as TYKi/TMPK2), which is crucial for the phosphorylation of dCMP and dUMP in mitochondria, was highly induced after DENV infection. As an IFN-inducible gene (Kennedy et al., 2015), CMPK2 is primarily localized in the mitochondria (Chen et al., 2008; Xu et al., 2008). To our surprise, after cloning of this molecule, published studies investigating CMPK2 roles and functions are very limited. A recently published study by El-Diwany et al. showed that IFN-mediated restriction of human HIV production can be attenuated by reduction of CMPK2 expression (El-Diwany et al., 2018). In addition, CMPK2 acts in concert with viperin-mediated production of ddhCTP during viral infection and ddhCTP functions as a chain terminator for the RNA-dependent RNA polymerases from multiple members of the *Flavivirus* genus, including DENV (Gizzi et al., 2018). A very insightful study conducted by Zhong et al. further revealed critical roles of CMPK2 in lipopolysaccharide (LPS)-induced inflammatory responses through activation of inflammasome pathway (Zhong et al., 2018). Altogether, these recently revealed messages highlight the possibility that CMPK2 may participate in DENV infection-mediated immune responses. Accordingly, the main goals of this study are to investigate the roles of CMPK2, highly upregulated in human DCs after DENV infection, in several mechanisms responsible for immunopathogenesis of DENV infection. The specific emphasis on several different aspects, including viral production, the immune reactions happening in mitochondrial machinery, and mediators and mechanisms responsible for antiviral immune responses, will be the target of the study.

In the present report, we demonstrated that CMPK2 not only preserves antiviral effects but also plays critical roles in several DENV infection-induced immune responses, such as mtROS production, 8-hydroxy-2′-deoxyguanosine (8-OHdG) production, mtDNA release into the cytosol, Toll-like receptor (TLR)-9 activation, inflammasome pathway activation, antiviral cytokine IFN-α/IFN-λ release, and cell migration. By examining mouse bone marrow-derived dendritic cells (BMDCs) from IFN-α receptor (IFN-αR) knockout (KO) and signal transducer and activator of transcription 1 (STAT1) KO mice, we further demonstrated that both IFN-dependent mechanisms and IFN-independent mechanisms contributed to CMPK2-mediated antiviral effects. The understanding of the extensive involvement of CMPK2 in DENV infection-induced immune responses is important for delineating how mitochondrial components are involved in the immune system defending against DENV infection and in DENV-mediated immunopathogenesis in humans.

RESULTS

CMPK2 induction and related signaling in DENV-infected cells

Microarray analysis revealed that CMPK2, among 20 listed mitochondria-associated genes, was highly induced in DENV-infected human DCs compared with mock-infected cells (Figures 1A and S1). Considering that in response to DENV infection, an immortalized cell line and primary cells may behave differently (Lai et al., 2018), both cell lines and primary cells were examined and sometimes compared side by side in individual experiments. In Figure 1B, we showed that CMPK2 mRNA induction could be widely observed in immortalized cell lines, such as the human macrophage cell line THP-1 and the lung epithelial cell line A549, and in both human primary cells and mouse primary cells, such as DCs (human DCs and mouse BMDCs) and macrophages (mouse bone marrow-derived macrophages [BMDMs]), after DENV infection. We could not detect the induction of CMPK2 mRNA expression in 293T cells. Induction of the CMPK2 protein, which was compatible with the induction of CMPK2 mRNA expression, was also observed in BMDCs and the THP-1 and A549 cell lines by western blotting (Figure 1C). By confocal microscopic examination, we showed that DENV-induced CMPK2 could be detected in both cytosol and mitochondria (Figure 1D). The induction of CMPK2 in NS3-negative cell suggests the presence of paracrine effect, likely from IFN stimulation. The results in Figure 1E revealed the presence of CMPK2 protein in both cytosolic and mitochondrial subfractions of DENV-infected A549 cells. The data suggest that after synthesis in the cytosol, CMPK2 quickly moved to the mitochondria and CMPK2 increased in both cytosolic and mitochondrial subfractions after DENV infection. Infection with four serotypes of DENV induced CMPK2 mRNA expression, although the intensity varied (Figure 1F). Because a variety of signaling pathways are involved in triggering immune response in DENV infection, we examined the potential pathways that regulate DENV-induced CMPK2 activation. Treatment of DENV-infected BMDCs with different chemical inhibitors examined with appropriate concentrations revealed that DENV-induced CMPK2 mRNA expression was dependent on JAK1/Tyk2 but not dependent or only weakly dependent on the other signaling molecules examined, such as phosphoinositide 3-kinases (PI-3K) and mitogen-activated protein kinases (MAPKs) (Figure S2A). Along with the inhibition of DENV-induced CMPK2 mRNA expression by the treatment with JAK1/Tyk2 inhibitors, the DENV-induced IFN-α mRNA decreased (Figure S2B) and DENV RNA increased (Figure S2C). Differential effects on CMPK2 mRNA, IFN-α mRNA, and DENV RNA expression were observed by the treatment of various chemical inhibitors in DENV-infected BMDCs (Figures S2A–S2C).

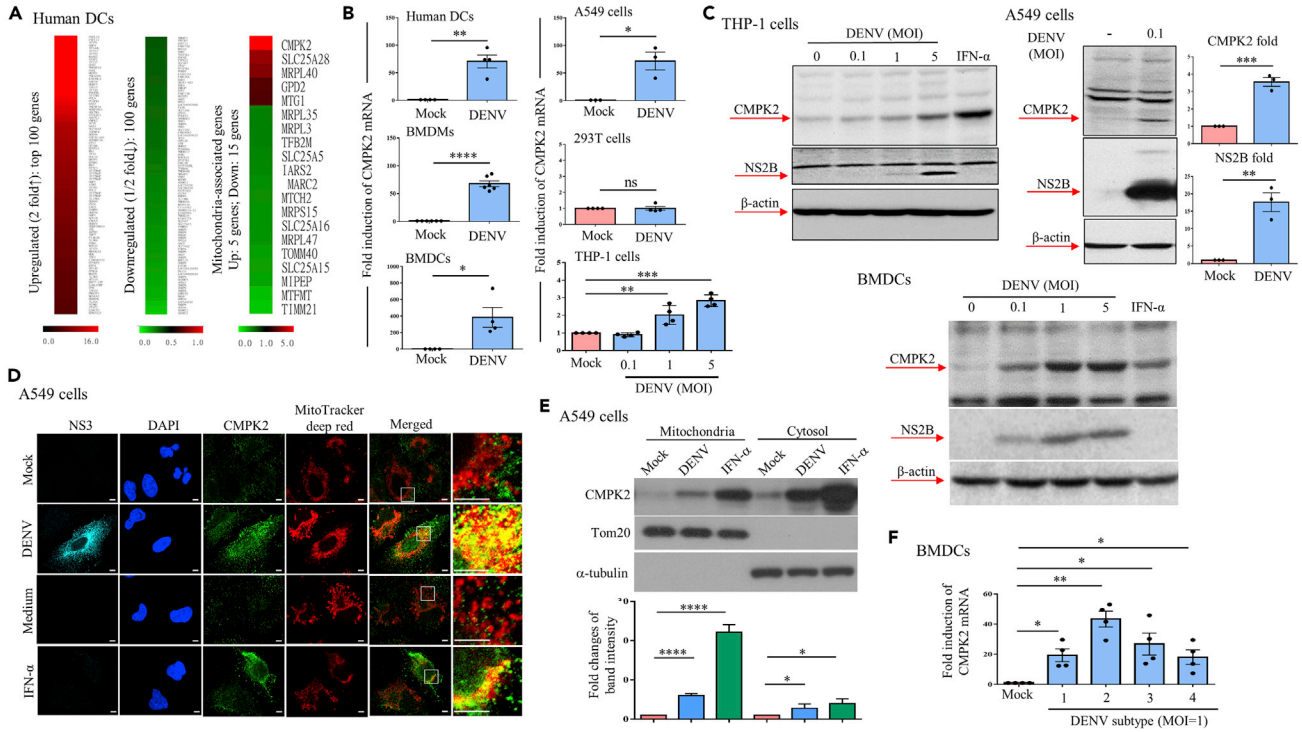

Figure 1. DENV infection induced CMPK2

(A–F) Human dendritic cells (DCs) were infected with DENV (MOI = 5) or mock infected for 24 h, and microarray analysis was conducted. Among the 20 listed mitochondria-associated genes, CMPK2 was the one most highly induced by DENV infection (A). Both human and mouse primary and immortalized cells, including human DCs, BMDCs, BMDMs, and the cell lines A549, 293T, and THP-1, were infected with DENV at an MOI of 1 (A549 and 293T), MOI of 5 (human DCs, BMDCs, and BMDMs), or different MOIs (THP-1 cells). THP-1 cells were infected for 72 h, and the other cells were infected for 24 h. The mRNA expression of CMPK2 was measured by qPCR (B). The protein levels of CMPK2 in THP-1 cells, BMDCs, and A549 cells infected with various MOIs of DENV or treated with IFN-α (100 U/mL) as indicated were determined by western blotting (C) and confocal microscopy with staining with an anti-CMPK2 antibody, MitoTracker Deep Red, anti-NS3, and DAPI (D). Scale bar, 5 μm. The CMPK2 protein was detectable in both cytosolic and mitochondrial subfractions of A549 cells infected by DENV (MOI = 1) (E). BMDCs infected with four different DENV serotypes were evaluated to measure the mRNA expression of CMPK2 (F). Values represent the mean of the individual measurements in each sample ±SEM. *p < 0.05, **p < 0.01, ***p < 0.001, and ****p < 0.0001. p value was calculated by the Student's t test (B, C, E, and F), except for THP-1 cells in (B) where one-way ANOVA was used for calculation.

Antiviral effects of CMPK2 in DENV infection

In the zebrafish model, CMPK2 preserved antiviral activity in Spring viraemia of carp virus-infected cells (Liu et al., 2019). In addition, the potential antiviral activity of CMPK2 was reported in the example of HIV infection (El-Diwany et al., 2018). To test whether CMPK2 preserves anti-DENV effects, BMDMs, BMDCs, and human DCs were examined. The results showed that knockdown (KD) of CMPK2 expression enhanced DENV RNA levels, suggesting that CMPK2 had antiviral effects on BMDMs (Figure 2A), BMDCs (Figure 2B) and human DCs (Figure 2C). To further examine the roles of CMPK2 in antiviral activity, A549 cells that did not constitutively express CMPK2 (Xu et al., 2008) were transfected with green fluorescent protein (GFP) control or CMPK2-GFP. The results showed that overexpression of CMPK2-GFP suppressed viral replication compared with the GFP control (Figure 2D), and the effect appeared to be dose-dependent (Figure 2E). Overexpression of CMPK2-GFP also inhibited viral NS3 protein expression, as determined by confocal microscopy examination (Figure S3). IFN-α-mediated antiviral effects were also reduced in CMPK2-KD A549 cells (Figure 2F). Similar to our previous observation in human DCs, DENV infection in BMDCs did not cause cell death (Figure 2G).

DENV-induced IFN but not TNF-α production was blocked in THP-1 cells with CMPK2 knocked out

To more clearly explore the roles of CMPK2, four CMPK2-KO THP-1 clones were generated by CRISPR-Cas9 approaches as described in experimental procedures. These CMPK2-KO clones contained different sequences leading to the early termination of CMPK2 protein production, except that both clone #3-7 and

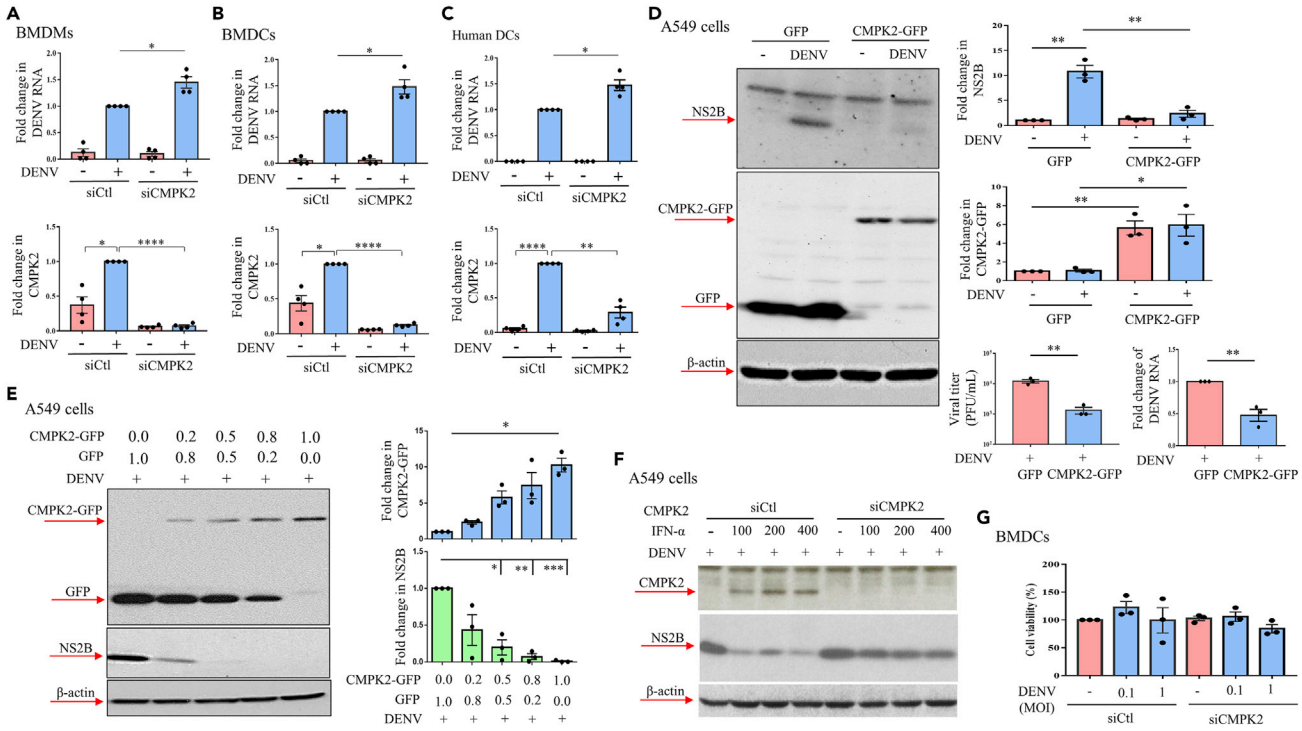

Figure 2. Impacts of CMPK2 knockdown or overexpression on DENV infection-induced effects

(A–G) BMDMs, BMDCs, or human DCs were treated with small interfering RNA (siRNA) targeting CMPK2 to KD the expression of CMPK2 or control siRNA. Cells were then infected with DENV (MOI = 0.1 for murine cells and MOI = 5 for human DCs) for 48 h (murine cells) or 24 h (human DCs), and viral RNA and CMPK2 mRNA levels were measured (A for BMDMs, B for BMDCs, and C for human DCs). A549 cells were transfected with CMPK2-GFP or a GFP control and then infected with DENV, and the expression of CMPK2-GFP and viral NS2B was measured by western blotting (D). A549 cells were transfected with different doses of CMPK2-GFP or the GFP control and then infected with DENV (MOI = 1) or left uninfected, and the expression of CMPK2-GFP and viral NS2B was measured by western blotting (E). A549 cells with CMPK2 KD by treatment with siRNA were infected with DENV (MOI = 1) in the presence or absence of different dosages of IFN-α as indicated. The expression of CMPK2 and viral NS2B was measured by western blotting (F). BMDCs infected with DENV for 48 h were collected, and cell survival was measured with a CCK-8 assay (G). Values represent the mean of the individual measurements in each sample ±SEM. *$p < 0.05$, **$p < 0.01$, ***$p < 0.001$, and ****$p < 0.0001$. p value was calculated by the Student's t test (A, B, C, D, and G) or one-way ANOVA (E).

clone #3-8 shared the same sequences (Figure 3A). DENV infection induced CMPK2 expression, whereas CMPK2 KO abolished these effects (Figure 3B). Additionally, CMPK2 KO also inhibited the induction of the mRNA and protein production of the major antiviral cytokines IFN-α and IFN-λ1 (Figure 3C) (Hsu et al., 2016). Similar results were also observed for the DENV-induced mRNA expression of IFN-α and IFN-λ2/3 in mouse BMDCs with CMPK2 knocked down via CMPK2-specific small interfering RNA (siRNA) introduction (Figure 3D). Interestingly, KD of CMPK2 expression did not affect the DENV-induced mRNA expression of tumor necrosis factor alpha (TNF-α) (Figure 3D). Differential regulation of DENV-induced antiviral and pro-inflammatory cytokines production was also demonstrated in human DCs by measuring protein levels with ELISA (Figure 3E). Subsequent studies showed that CMPK2 deficiency did not affect DENV-induced phosphorylation of p65 in THP-1 cells (Figure 3F) and BMDCs (Figure 3G). The results may explain in part why the deficiency of CMPK2 only affected DENV-induced IFN but not pro-inflammatory cytokine production. A recently published report demonstrating that C-type lectin member 18A (CLEC18A) enhances the production of type I and type III IFNs, but not proinflammatory cytokines, in response to H5N1 influenza A virus infection may serve as another example (Huang et al., 2021).

Deficiency in CMPK2 attenuated DENV-induced mtDNA release and TLR9 activation

Given the critical role of mitochondria in immune response, the release of mtDNA into the cytoplasm activates several different pattern recognition receptors and cytosolic DNA sensors such as the cyclic GMP-AMP synthase-stimulator of interferon genes (cGAS-STING) and TLR9 and induces type I IFN responses (Riley and Tait, 2020). We previously showed that DENV infection induces the release of mtDNA into the cytosol, where it binds to Toll-like receptor 9 (TLR9) and induces a potent inflammatory response (Lai et al., 2018). We

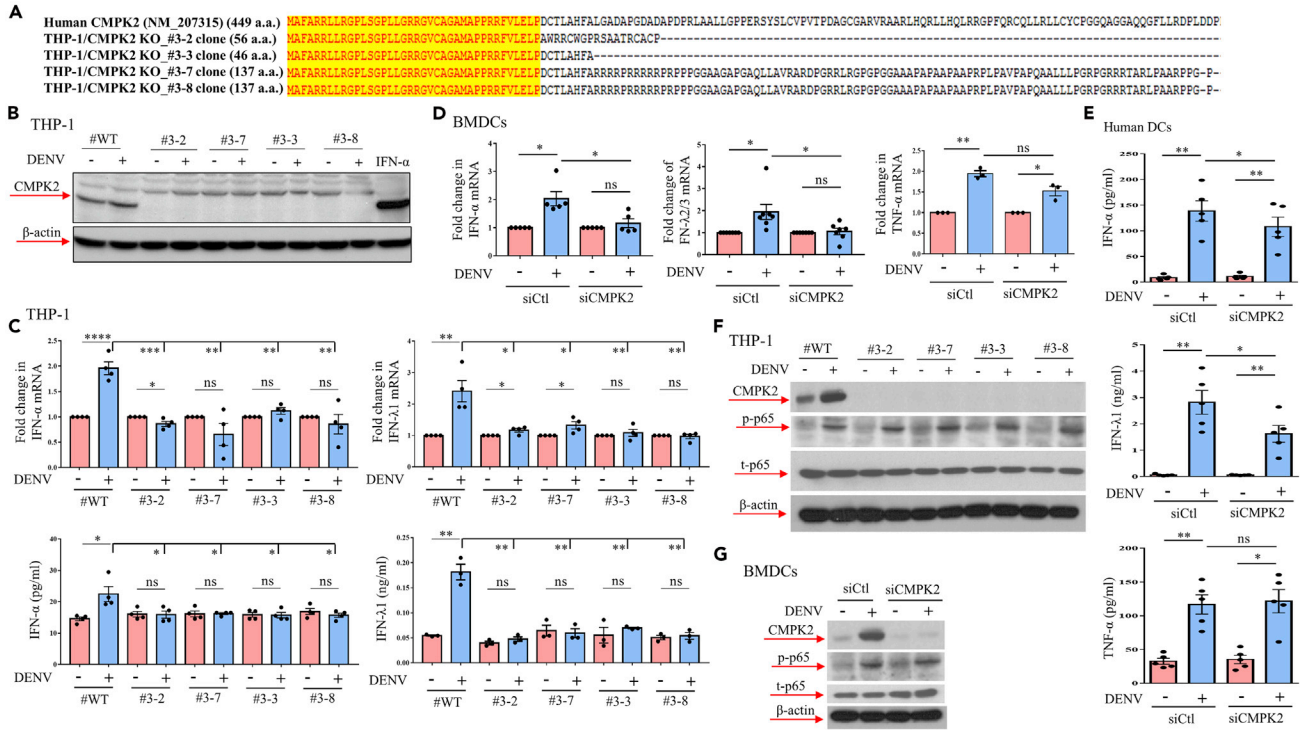

Figure 3. Effects of CMPK2 knockout in the context of DENV infection

(A–G) Four THP-1 CMPK2-KO clones were generated with CRISPR-Cas9 approaches as described in experimental procedures (A). DENV infection (MOI = 5) failed to induce the protein expression of CMPK2 in all CMPK2-KO clones; IFN-α treatment served as a positive control (B). The DENV infection-induced mRNA and protein expressions of both IFN-α and IFN-λ1 were evaluated in wild-type cells and CMPK2-KO clones (C). The mRNA levels of IFN-λ2/3, IFN-α, and tumor necrosis factor alpha (TNF-α) were measured in BMDCs with or without CMPK2 KD infected with DENV (MOI = 1) for 24 h (D). Human DCs treated with siCtl or siCMPK2 were infected by DENV (MOI = 5) for 24 h, and the supernatants were collected for measuring IFN-α, IFN-λ1, and TNF-α protein concentrations with ELISA (E). THP-1 and four THP-1 CMPK2-KO clones (F) and BMDCs (G) were infected by DENV (MOI = 5 for THP-1 and MOI = 1 for BMDCs), and the expression of CMPK2, un-phosphorylated, and phosphorylated p65 were measured by western blots. Values represent the mean of the individual measurements in each sample ±SEM. The representative results from two independent experiments were shown (F and G). *$p < 0.05$, **$p < 0.01$, ***$p < 0.001$, and ****$p < 0.0001$. p value was calculated by the Student's t test (C, D, and E).

wondered whether CMPK2 participates in these events. The results showed that DENV infection specifically increased cytosolic mtDNA levels, whereas the total amount of mtDNA remained unchanged after DENV infection. In addition, CMPK2 KO significantly abolished DENV-induced mtDNA release into the cytosol (Figure 4A). An examination of BMDCs also confirmed this effect, which showed that CMPK2 KD reduced DENV-induced mtDNA release into the cytosol (Figure 4B). DENV infection induced the expression of TLR-9 at both the mRNA and protein levels, whereas the effects were significantly attenuated by CMPK2 KD (Figure 4C). A similar result was observed for CMPK2-KO THP-1 clones (Figure 4D). 8-OHdG, an important biomarker for measuring the effect of endogenous oxidative damage to DNA, was measured by flow cytometry to clarify the oxidation status of mtDNA in DENV-infected cells. The results revealed an increased amount of the oxidized form of DNA after DENV infection, and the effect was attenuated after KD of CMPK2 expression in BMDCs (Figure 4E). The inhibition of DENV-induced 8-OHdG expression was also confirmed by confocal microscopy (Figure 4F). Figure 4G showed that DENV-induced 8-OHdG production was also suppressed by knocking down CMPK2 expression in human DCs.

Deficiency in CMPK2 attenuated DENV-induced mtROS production and inflammasome pathway

Several intracellular stress pathways, including oxidative stress, unfolded protein response, and stress granules assembly are triggered along the processes of viral recognition and synthesis of viral genome and viral proteins (Valadao et al., 2016). In addition, infection with DENV induces the production of ROS (Lai et al., 2018), and the mitochondrial protein CMPK2 may contribute to these events. As shown in Figure 5A, DENV infection-induced mtROS production was suppressed in CMPK2-deficient KO clones. A

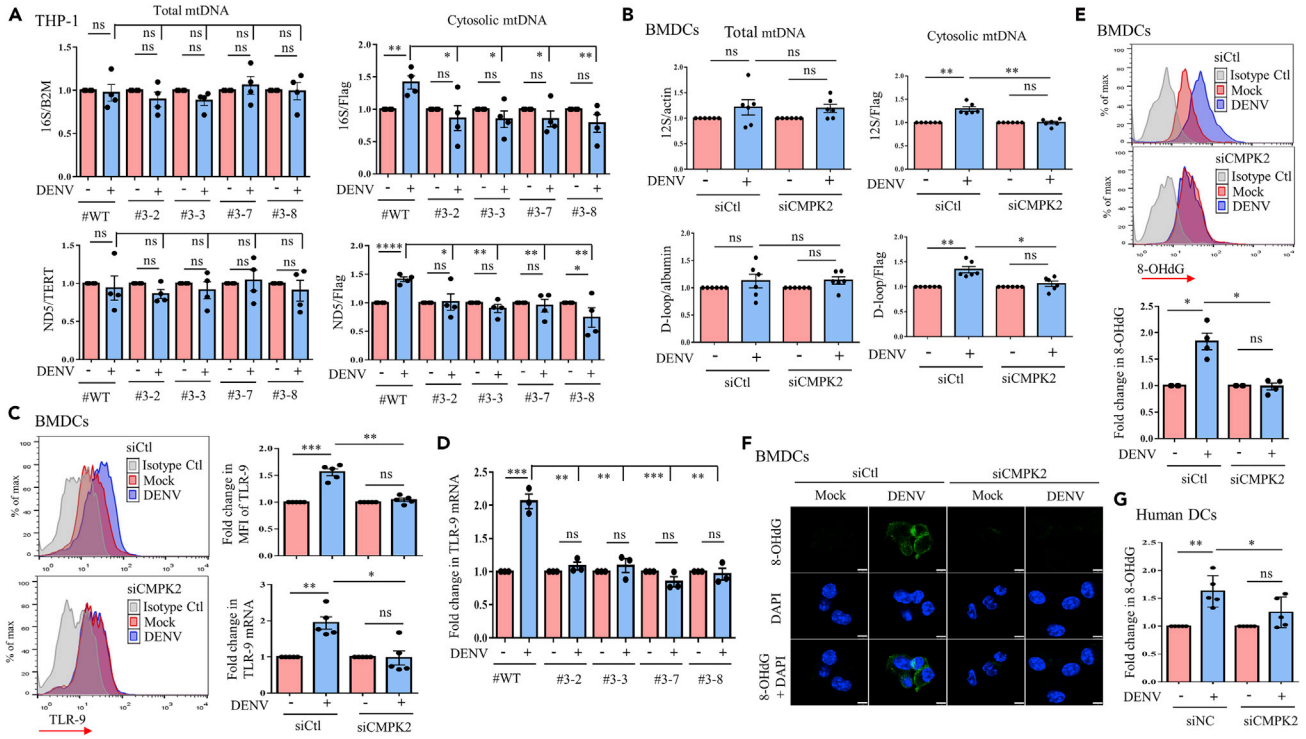

Figure 4. Effects of CMPK2 KO on the DENV infection-induced release of mtDNA and activation of TLR9

(A–G) THP-1 cells and THP-1 CMPK2-KO clones were infected with DENV (MOI = 5), and the levels of total mtDNA and cytosolic mtDNA were measured by qPCR (A). Both 16S levels and ND5 levels were normalized to nuclear DNA (actin or albumin as indicated) or the exogenously introduced FLAG level. BMDCs treated with control siRNA or CMPK2-specific siRNA were infected with DENV (MOI = 1), and the levels of total and cytosolic mtDNA were measured by qPCR (B). Both 12S levels and D-loop levels were normalized to nuclear DNA (B2M or TERT) or the exogenously introduced FLAG level. The intensity of TLR9 expression in BMDCs treated with CMPK2-specific siRNA or control siRNA was determined by flow cytometry (C). The mRNA expression of TLR9 in wild-type cells and CMPK2-KO clones was determined by qPCR (D). The knockdown of CMPK2 expression in BMDCs also resulted in a reduction in the DENV infection-induced expression of 8-OHdG measured by flow cytometry (E) and confocal microscopy (F). Scale bar, 5 μm. Similarly, knockdown of CMPK2 expression reduced DENV-induced 8-OHdG expression in human DCs (G). Values represent the mean of the individual measurements in each sample ±SEM. *$p < 0.05$, **$p < 0.01$, and ***$p < 0.001$. p value was calculated by the Student's t test (A, B, C, D, E, and G).

similar result was also observed when DENV-infected BMDCs were examined (Figure 5B). In addition, DENV-induced mtROS production was downregulated when CMPK2 expression was decreased in human DCs (Figure 5C). Given that the release of mtROS has been shown to be associated with the activation of inflammasome pathway (Zhong et al., 2018), subsequent experiments showed that DENV infection induced the release of mature interleukin (IL)-1 into the supernatant, and this effect was blocked in CMPK2-KO clones (Figure 5D). The measurement of IL-1β concentrations supported a similar conclusion (Figure 5E). Using BMDCs, we reproducibly observed the inhibitory effect of CMPK2-KD in DENV-induced IL-1β protein (Figure 5F). The same conclusion was reached by measuring IL-1β protein with ELISA in human DCs (Figure 5G). The activation of inflammasome pathway and the effects of CMPK2 KO and KD in THP-1 cells and BMDCs, respectively, were also confirmed by determining active caspase-1 expression by flow cytometry analysis (Figures S4A and S4B).

CMPK2 regulated DENV-induced cell migration

Migration of virus-infected cells to secondary lymphoid organs and their subsequent interaction with other immune effector cells is a crucial step in the onset of adaptive immunity (Yan et al., 2019). We previously showed that DENV infection induces human DC migration (Wu et al., 2009). To determine whether CMPK2 plays a role in this process, CMPK2-KO THP-1 clone #3-2 was mock infected or infected with DENV and chemotaxis assays were performed. The results showed that knocking out CMPK2 abolished DENV-induced cell migration (Figure S5A). The effects correlated with the reduced CCR7 mRNA expression in CMPK2-KO cells (Figure S5B). The determination of CCR7 protein expression by flow cytometry also confirmed this observation (Figure S5C). In parallel, results showed that knocking down CMPK2

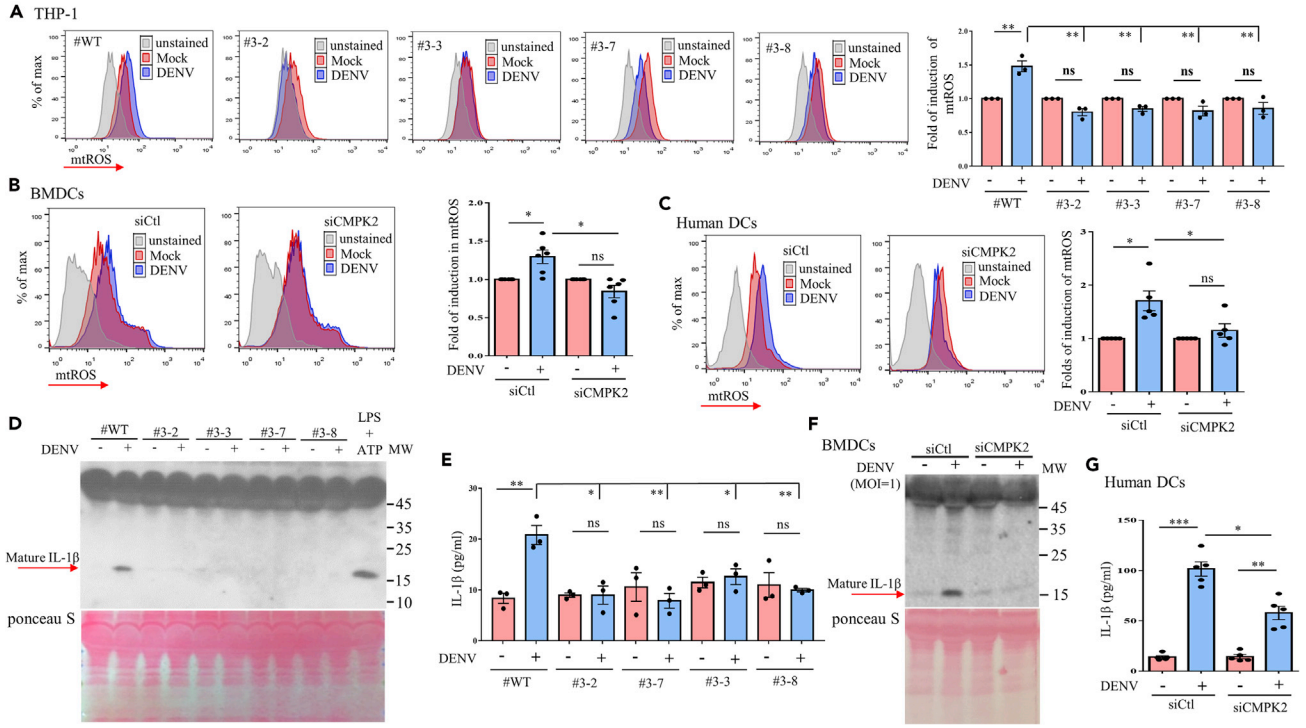

Figure 5. Effects of CMPK2 KO on DENV infection-induced mitochondrial superoxide production and inflammasome pathway

(A–G) THP-1 cells and THP-1 CMPK2-KO clones were infected with DENV (MOI = 5), and the levels of mtROS production measured by staining with MitoSOX were analyzed with flow cytometry (A). The production of mtROS in BMDCs transfected with control siRNA or CMPK2-specific siRNA and then infected with DENV (MOI = 1) was determined by flow cytometry (B). The effect of CMPK2 knockdown on DENV-induced mtROS production in human DCs was also determined (C). THP-1 cells and THP-1 CMPK2-KO clones were infected with DENV, and the levels of mature IL-1β in the supernatant were measured by western blotting (D) and ELISA (E). Additionally, the protein and mRNA expression of IL-1β in BMDCs transfected with control siRNA or CMPK2-specific siRNA and then infected by DENV was determined by western blotting (F). The effect of CMPK2 knockdown on DENV-induced IL-1β protein production in human DCs was examined with ELISA (G). Values represent the mean of the individual measurements in each sample ±SEM. *$p < 0.05$ and **$p < 0.01$. p value was calculated by the Student's t test (A, B, C, E, and G).

expression in BMDCs reduced DENV-induced chemotactic activity in chemotaxis assays (Figure S5D), CCR7 mRNA expression in a qPCR assay (Figure S5E), and the CCR7 protein level in a flow cytometry assay compared with treatment with control siRNA (Figure S5F).

Effects of CMPK2 on BMDCs from IFN-αR-KO and STAT1-KO mice

To further address the relationship between CMPK2 and IFN-α, BMDCs from IFN-αR-KO and STAT1-KO mice were prepared and examined. The results showed that DENV-induced CMPK2, STAT1, and phosphorylated STAT1 were abolished in BMDCs from both IFN-αR-KO mice and STAT1-KO mice compared with those from wild-type mice (Figure 6A). In contrast, DENV-induced NS2B protein expression was enhanced (Figure 6A). Additionally, the expression of CMPK2 mRNA and DENV RNA was decreased and enhanced, respectively, in BMDCs from both IFN-αR-KO mice and STAT1-KO mice compared with those from wild-type mice (Figure 6B). Furthermore, DENV-induced mtROS production was not detected in BMDCs from either IFN-αR-KO or STAT1-KO mice compared with those from wild-type mice (Figure 6C). DENV-induced 8-OHdG production was significantly suppressed in the absence of IFN-αR or STAT1 (Figure 6D). In accordance, DENV infection-induced mtDNA release into the cytosol was significantly reduced in the absence of either IFN-αR or STAT1 (Figure 6E). In supportive, DENV-induced IFN production was significantly reduced in BMDCs from IFN-αR-KO or STAT1-KO mice compared with those from wild-type mice (Figure S6).

Dependency of IFN-α on CMPK2-mediated antiviral activity

Because CMPK2 is one of the IFN-stimulated genes and KD or KO of CMPK2 suppresses DENV-induced IFN production, we wondered whether CMPK2 by itself can mediate any antiviral activity in the absence of IFN-α. CMPK2 was overexpressed in BMDCs from wild-type or IFN-αR-KO mice, and several effects

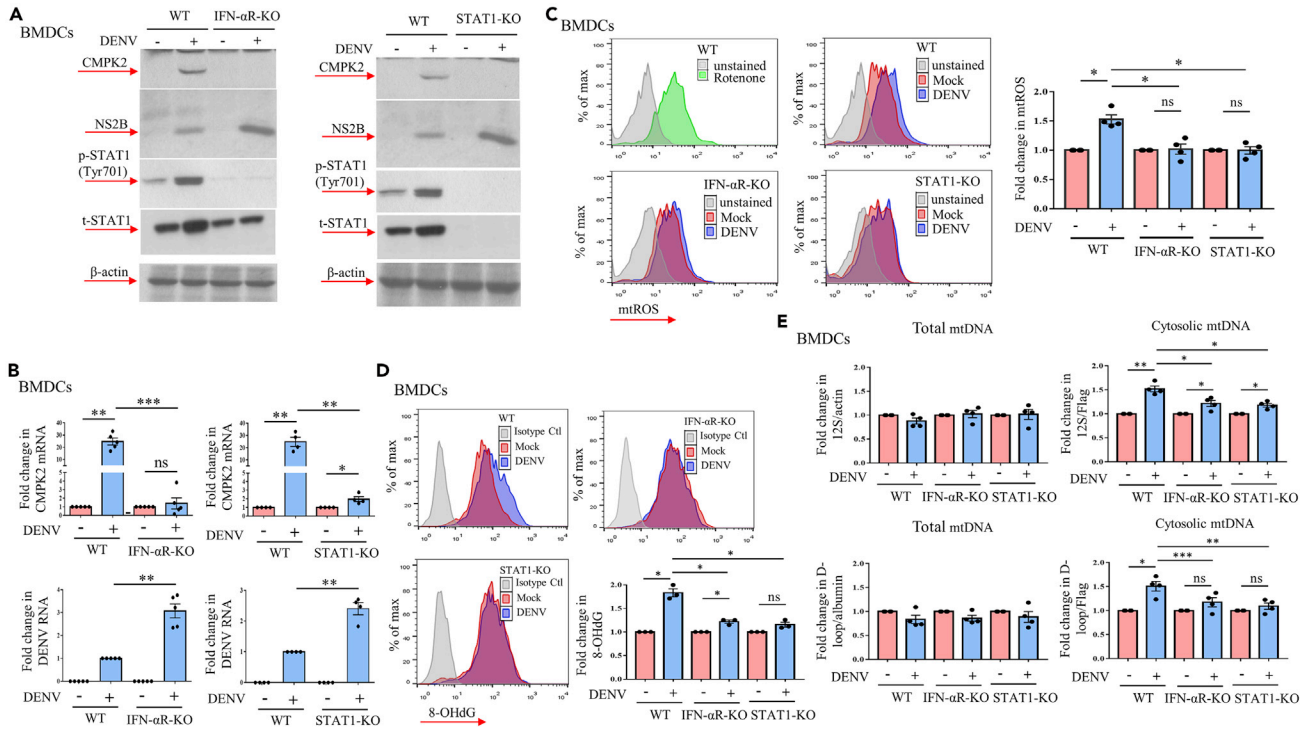

Figure 6. The effects of IFN-α receptor or STAT1 KO on DENV-induced CMPK2 expression and related events

(A–E) BMDCs were prepared from mice with KO of IFN-αR or STAT1 or control mice. Cells were then infected with DENV (MOI = 1), and the expression of CMPK2, NS2B, phosphorylated STAT1, total STAT1, IRF1, and β-actin was measured by western blotting (A). The expression of CMPK2 mRNA and DENV RNA was determined by qPCR (B). In addition, the production of mtROS (C) and 8-OHdG (D) was measured. Similar to Figure 4, the effects of IFN-αR or STAT1 KO on DENV-induced mtDNA release into the cytosol were determined in BMDCs (E). Values represent the mean of the individual measurements in each sample ±SEM. *p < 0.05, **p < 0.01, and ***p < 0.001. p value was calculated by the Student's t test (B, C, D, and E).

were subsequently examined. As shown in Figure 7A-1, overexpression of CMPK2-DYK was successfully achieved in BMDCs from wild-type and IFN-αR-KO mice. The results showed that overexpression of CMPK2 enhanced IFN-α (Figure 7A-2) and IFN-λ2/3 mRNA (Figure 7A-3) expression in wild-type and IFN-αR-KO cells, although IFN-αR deficiency attenuated DENV-induced IFN mRNA expression (Figures 7A-2 and 7A-3). Consistent with the results in Figure 2 showing that overexpression of CMPK2 suppressed viral loads, the CMPK2-mediated suppression of DENV RNA expression remained detectable in the absence of IFN-αR, suggesting the presence of an IFN-α-independent mechanism of CMPK2-mediated antiviral activity (Figure 7A-4). By measuring the level of the viral NS1 protein, we confirmed that CMPK2-mediated antiviral effects could be independent of IFN-α (Figure 7B showing different analysis with both the measurement of mean fluorescence intensity and the percentages of positive cells). Figure 7C shows the comparable transduction efficiency for BMDCs treated with a lentivirus encoding DYK or CMPK2-DYK. Although differentiation of monocytes into macrophages may activate CMPK2 (Chen et al., 2008), neither CMPK2 overexpression nor IFN-αR KO affected the phenotype of BMDCs (Figures 7D and S7). The several effects demonstrated in this report were combined into a cartoon illustrating the roles of CMPK2 in DENV-infected cells (Figure S8).

DISCUSSION

The major interests of this study are to investigate how the mitochondrial protein CMPK2 that was highly upregulated in human DCs after DENV infection can regulate different aspects of immune reactions in DENV-infected cells. After infection by DENV, DCs migrate from the bloodstream or peripheral tissues to the lymphoid organs where they can efficiently interact with and deliver signals to T cells and induce adaptive immunity. Along these processes, many intracellular and extracellular immunological events are occurring in DENV-infected cells and the bystander cells. Mitochondria are the major participants in these immunological events. Accordingly, we focused on investigating the eminent immune responses happening in DENV-infected cells, including viral replication, the production of antiviral and

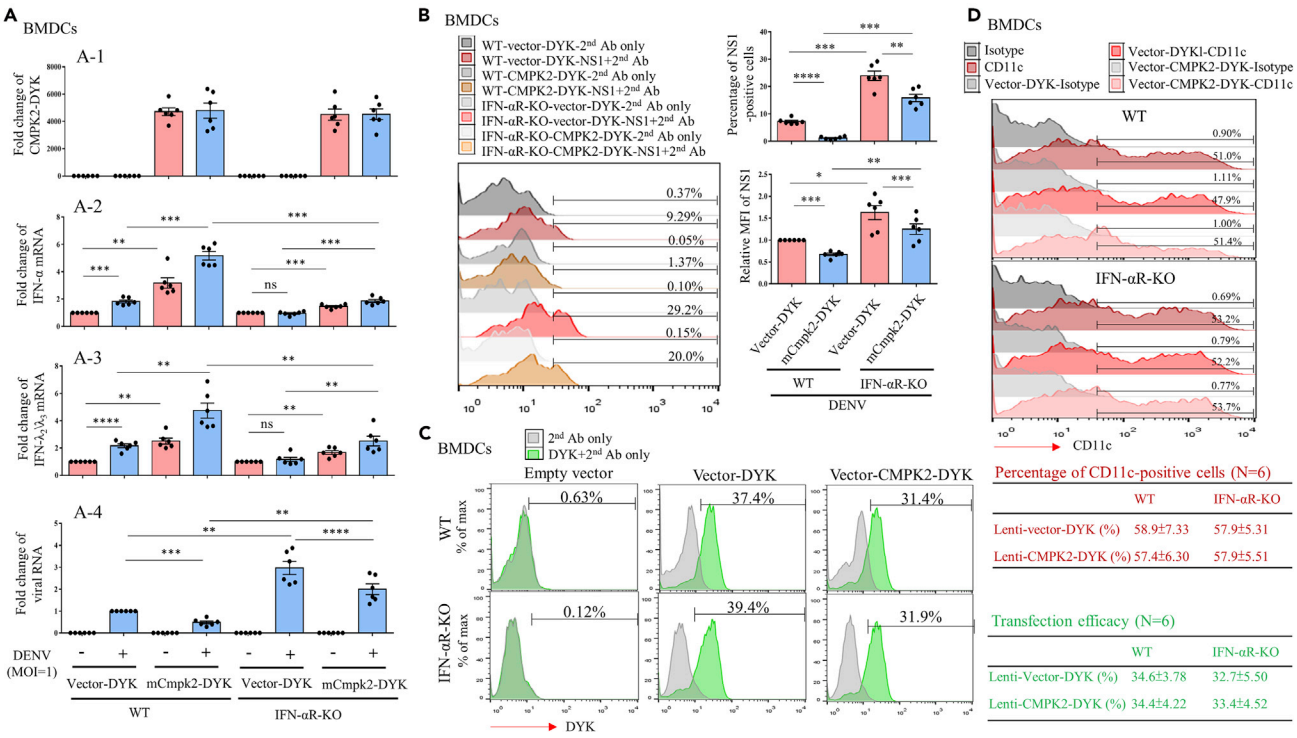

Figure 7. Overexpression of CMPK2 partially restored the antiviral effect of BMDCs from IFN-αR-KO mice

(A–D) BMDCs prepared from mice with IFN-αR knocked out or control mice were transfected with a lentivirus carrying DYK or CMPK2-DYK, and the cells were then infected with DENV (MOI = 1). The expression of DENV RNA, CMPK2 mRNA, IFN-α mRNA, and IFN-λ2/λ3 mRNA was determined by qPCR (A). Additionally, the levels of DENV NS1 protein expression were determined by flow cytometry, and the percentages of NS1-positive cells and the relative mean fluorescence intensity (MFI) of NS1 are presented individually (B). (C) The transduction efficiency from six independent experiments is shown. The percentages of CD11c-positive cells after transfection with DYK or CMPK2-DYK were measured by flow cytometry (D). Analysis of six independent experiments was performed. Values represent the mean of the individual measurements in each sample ±SEM. *p < 0.05, **p < 0.01, ***p < 0.001, and ****p < 0.0001. p value was calculated by the Student's t test (A, B, C, and D).

proinflammatory cytokines, the cell migration-associated mechanisms, and the triggering of mitochondrial machinery such as the production of mitochondrial ROS and the release of mitochondrial DNA into cytosol.

In response to DENV infection, several distinctive features can be observed in primary cells, mainly dendritic cells, compared with the commonly studied target cell lines, such as hepatoma cells, lung epithelial cells, and human embryonic kidney cells (Lai et al., 2018). A characteristic difference is the death response observed in DENV-infected cell lines but not in DENV-infected human DCs or DENV-infected BMDCs (Figure 2F). Accordingly, the inclusion of cell lines and primary cells and even cells from humans and mice in this report is of particular significance. In identifying the critical molecule that is tightly associated with the mitochondria, microarray analysis led to the discovery that CMPK2 is greatly induced after DENV infection. Although CMPK2 was cloned more than 10 years ago, the roles of CMPK2 remain largely unclear. We thus performed an extensive analysis to characterize the roles of CMPK2 in DENV infection. To our surprise, except the DENV infection-induced production of TNF-α and IL-6 (Figures 3D and 3E and data not shown), the mitochondrial protein CMPK2 participates in and regulates most of the DENV infection-induced immune responses examined in this study. Interestingly, CMPK2 did not affect DENV-induced nuclear factor-κB activation. When we examined several potential upstream molecules regulating DENV-induced CMPK2 activation, the results suggested that the DENV infection-induced activation of CMPK2 was critically dependent on IFN-α downstream molecules because inhibitors of JAK2 and Tyk2 potently suppressed DENV-induced CMPK2 activation. In contrast, inhibitors targeting PI-3K and MAPK seemed to be ineffective in this aspect. Early studies showed that CMPK2 is mainly expressed in hematopoietic and lymphoid cells but is not detected in cells enriched in mitochondria, such as cells in the muscles and heart, by northern blot analysis (Xu et al., 2008). This suggests that CMPK2 may not play major roles in metabolism but rather may be critical in regulating hematolymphoid function or homeostasis.

As a mitochondrial protein, CMPK2 is critical in DENV-induced mitochondrial operations, such as the release of fragmented mtDNA from the mitochondria into the cytosol; however, CMPK2 did not affect the total level of mtDNA, which was also not increased by DENV infection, as shown in our previous study (Lai et al., 2018). The effect of DENV infection is somewhat different from that of stimulation with LPS, which not only results in an increase in mtDNA synthesis but also is inhibited by CMPK2-specific small hairpin RNA (shRNA) treatment (Zhong et al., 2018). Released mtDNA binds to cyclic GMP-AMP synthase (cGAS) and mediates the immune response; however, this effect is hampered by virus-mediated protection (Aguirre et al., 2017). In addition to binding to cGAS, mtDNA may bind to TLR-9; this participation is a rare example of TLR-9 involvement in immune responses triggered by an RNA virus, such as DENV (Lai et al., 2018). Following the activation of TLR-9, many consequences, such as the production of mtROS and generation of 8-OHdG, can be observed, and these effects can be hampered by CMPK2 deficiency. Interestingly, the NLRP3 activator-induced production of mtROS remains unaffected in cells treated with CMPK2-specific shRNA (Zhong et al., 2018). Furthermore, the activation of the inflammasome pathway by DENV infection was also suppressed by CMPK2 deficiency. Surprisingly, we did not detect a change in the mitochondrial membrane potential in DENV-infected THP-1 cells (data not shown), a phenomenon compatible with our earlier observation in human dendritic cells (Lai et al., 2018). These results suggest that the activators of CMPK2 are diverse and that depending on target cell identity, CMPK2 downstream effects can vary.

Using THP-1 cells, El-Diwany et al. observed that IFN-mediated inhibition of HIV replication was significantly reduced in cells transfected with CMPK2-specific siRNA compared with cells transfected with control scrambled siRNAs (El-Diwany et al., 2018). In support of the observation by El-Diwany et al. (2018), furthermore, we showed that the expression of DENV RNA increased in BMDCs with knockdown of CMPK2 expression and that overexpression of CMPK2 suppressed DENV NS2B expression and viral production in a dose-dependent manner. This conclusion was supported by an alternative approach of confocal microscopy evaluation of DENV NS2B protein levels. Given that knockdown of CMPK2 expression attenuated IFN-α-mediated antiviral effects, our study further suggests that CMPK2 not only regulated DENV-induced IFN-α and IFN-λ production but also participated in IFN-α-mediated antiviral activity. Moreover, studies using primary cells from both IFN-αR-KO mice and STAT1-KO mice confirmed that overexpression of CMPK2 in the absence of IFN-α or STAT1 could still mediate antiviral activity, suggesting an IFN-independent antiviral effect of CMPK2. The regulation of DENV-induced production of IL-1β, an activator of IFN and IFN-associated antiviral signals (Aarreberg et al., 2019), by CMPK2 also partially accounts for the antiviral activity of this molecule.

It has been shown that CMPK2 catalyzes the phosphorylation of CMP, UMP, dCMP, and dUMP by ATP to the corresponding diphosphates (Chen et al., 2008; Xu et al., 2008). The role of CMPK2 in immunomodulatory and antiviral effects might involve its enzymatic function in altering these nucleotide pools produced in mitochondria. Of note, studies have suggested that the increase of uracil in viral genomic DNA intermediates during replication plays a part in the innate immune system to fight against virus infection (Sire et al., 2008). For example, by increasing the cellular dUTP:dTTP ratio that promotes dUTP incorporation, uracilation of retroviral genomes limits viral replication and appears to be one of the mechanisms for innate immunity to fight against HIV infection (Weil et al., 2013). Another line of evidence has demonstrated that viperin, which is co-stimulated with CMPK2 in response to infection signal, restricts viral RNA replication due to their cooperation in the conversion of CMP to 3′-deoxy-3′,4′-didehydro-CTP (ddhCTP), a chain terminator for viral RNA polymerases (Bernheim et al., 2020; Gizzi et al., 2018). Along these established findings, it is highly possible that the enzymatic function of CMPK2 in host cells is involved in defending against DENV infection. However, the underlying mechanism remains to be investigated.

One critical event that DENV-infected patients may experience is cytokine storm, which may result in fatal manifestations such as DHF and DSS. Many potential mechanisms and effects have been reported, and CMPK2 seems to regulate some of these processes, such as activation of the mitochondrial machinery, cell migration, and activation of the inflammasome pathway. Although the participation of CMPK2 in hyperactivated DENV-induced immune responses may have unwanted effects on DENV-infected patients, a reduction or deficiency in CMPK2 expression may also greatly suppress antiviral immunity, as discussed above, by both reducing the production of the antiviral cytokines IFN-α and IFN-λ and decreasing the direct antiviral activity of CMPK2. Whether CMPK2 may serve as a useful therapeutic target for the treatment of DENV infection needs to be investigated using animal systems. The present studies, through various and broad approaches, demonstrated the critical roles of CMPK2 in DENV infection-induced immune responses. Our studies further identify critical roles for the mitochondria and their components in regulating the immune responses triggered by DENV infection.

Limitations of the study

Given that both genetic KD and KO approaches have been undertaken to address the roles of CMPK2, the use of cells from CMPK2-KO animals should provide much stronger and solid evidence supporting the roles of this molecule. Furthermore, the introduction of DENV into CMPK2-KO animals and the determination of animal survival and viral load should give definitive answers as to whether CMPK2, also an IFN-inducible gene, is critical to protect DENV infection. As a mitochondrial protein, how CMPK2 may regulate the metabolic processes and mediate its antiviral reactions was not addressed in this study. These limitations raise few interesting directions for the ongoing studies exploring the roles and mechanisms that CMPK2 may play in DENV and other virus infection-mediated immunological and nonimmunological responses.

STAR★METHODS

Detailed methods are provided in the online version of this paper and include the following:

- KEY RESOURCES TABLE
- RESOURCE AVAILABILITY
  - Lead contact
  - Materials availability
  - Data and code availability
- EXPERIMENTAL MODEL AND SUBJECT DETAILS
  - Cell culture and reagents
  - DENV preparation and infection
  - Preparation of human monocyte-derived dendritic cells and mouse bone marrow-derived macrophages (BMDMs) and bone marrow-derived dendritic cells (BMDCs)
- METHOD DETAILS
  - Preparation of cytosolic and mitochondrial fraction
  - siRNA transfection
  - CMPK2-knockout THP-1 cells
  - Overexpression of CMPK2 in BMDCs and A549 cells
  - Quantitative RT-qPCR
  - Extraction of total and cytosolic DNA and mtDNA measurement
  - Western blotting
  - Flow cytometry
  - Measurement of mitochondrial ROS levels
  - Determination of cytokine concentrations via ELISA
  - CCK-8 cell viability assay
  - Immunofluorescence staining and confocal imaging
  - Caspase 1 activity assay
  - Chemotaxis assay
- QUANTIFICATION AND STATISTICAL ANALYSIS

SUPPLEMENTAL INFORMATION

Supplemental information can be found online at https://doi.org/10.1016/j.isci.2021.102498.

ACKNOWLEDGMENTS

We thank Dr. Y.L. Lin (Academic Sinica, Taipei, Taiwan) for providing different serotypes of DENV strains. This work was supported by grants from the Ministry of Science and Technology (MOST 107-2314-B-182A-132-MY3 to J.-H.L. and 109-2314-B-400-035 to L.-J.H.) and Chang Gung Memorial Hospital (CMRPG1H0101), Taiwan, R.O.C.

AUTHOR CONTRIBUTIONS

J.-H.L. and L.-J.H. participated in the study design. D.-W.W, C.-H.W., L.-F.H., and C.-Y.H. performed the experiments and analyzed the data. S.-M.K., A.C., and Z.-F.C. provided various tools and reagents for the study and joined data discussion. L.-J.H. and J.-H.L. analyzed the data and wrote the report. All authors read and approved the manuscript.

DECLARATION OF INTERESTS

The authors confirm that there are no conflicts of interest.

Received: December 7, 2020
Revised: March 31, 2021
Accepted: April 28, 2021
Published: June 25, 2021

REFERENCES

Aarreberg, L.D., Esser-Nobis, K., Driscoll, C., Shuvarikov, A., Roby, J.A., and Gale, M., Jr. (2019). Interleukin-1beta induces mtDNA release to activate innate immune signaling via cGAS-STING. Mol. Cell *74*, 801–815.e6.

Aguirre, S., Luthra, P., Sanchez-Aparicio, M.T., Maestre, A.M., Patel, J., Lamothe, F., Fredericks, A.C., Tripathi, S., Zhu, T., Pintado-Silva, J., et al. (2017). Dengue virus NS2B protein targets cGAS for degradation and prevents mitochondrial DNA sensing during infection. Nat. Microbiol. *2*, 17037.

Bernheim, A., Millman, A., Ofir, G., Meitav, G., Avraham, C., Shomar, H., Rosenberg, M.M., Tal, N., Melamed, S., Amitai, G., et al. (2020). Prokaryotic viperins produce diverse antiviral molecules. Nature *589*, 120–124.

Bonilla, D.L., Bhattacharya, A., Sha, Y., Xu, Y., Xiang, Q., Kan, A., Jagannath, C., Komatsu, M., and Eissa, N.T. (2013). Autophagy regulates phagocytosis by modulating the expression of scavenger receptors. Immunity *39*, 537–547.

Castro, M.C., Wilson, M.E., and Bloom, D.E. (2017). Disease and economic burdens of dengue. Lancet Infect. Dis. *17*, e70–e78.

Chatel-Chaix, L., Cortese, M., Romero-Brey, I., Bender, S., Neufeldt, C.J., Fischl, W., Scaturro, P., Schieber, N., Schwab, Y., Fischer, B., et al. (2016). Dengue virus perturbs mitochondrial morphodynamics to Dampen innate immune responses. Cell Host Microbe *20*, 342–356.

Chen, Y.L., Lin, D.W., and Chang, Z.F. (2008). Identification of a putative human mitochondrial thymidine monophosphate kinase associated with monocytic/macrophage terminal differentiation. Genes Cells *13*, 679–689.

El-Diwany, R., Soliman, M., Sugawara, S., Breitwieser, F., Skaist, A., Coggiano, C., Sangal, N., Chattergoon, M., Bailey, J.R., Siliciano, R.F., et al. (2018). CMPK2 and BCL-G are associated with type 1 interferon-induced HIV restriction in humans. Sci. Adv. *4*, eaat0843.

Gizzi, A.S., Grove, T.L., Arnold, J.J., Jose, J., Jangra, R.K., Garforth, S.J., Du, Q., Cahill, S.M., Dulyaninova, N.G., Love, J.D., et al. (2018). A naturally occurring antiviral ribonucleotide encoded by the human genome. Nature *558*, 610–614.

Ho, L.J., Hung, L.F., Weng, C.Y., Wu, W.L., Chou, P., Lin, Y.L., Chang, D.M., Tai, T.Y., and Lai, J.H. (2005). Dengue virus type 2 antagonizes IFN-alpha but not IFN-gamma antiviral effect via down-regulating Tyk2-STAT signaling in the human dendritic cell. J. Immunol. *174*, 8163–8172.

Hsu, Y.L., Wang, M.Y., Ho, L.J., and Lai, J.H. (2016). Dengue virus infection induces interferon-lambda1 to facilitate cell migration. Sci. Rep. *6*, 24530.

Huang, Y.L., Huang, M.T., Sung, P.S., Chou, T.Y., Yang, R.B., Yang, A.S., Yu, C.M., Hsu, Y.W., Chang, W.C., and Hsieh, S.L. (2021). Endosomal TLR3 co-receptor CLEC18A enhances host immune response to viral infection. Commun. Biol. *4*, 229.

Kennedy, W.P., Maciuca, R., Wolslegel, K., Tew, W., Abbas, A.R., Chaivorapol, C., Morimoto, A., McBride, J.M., Brunetta, P., Richardson, B.C., et al. (2015). Association of the interferon signature metric with serological disease manifestations but not global activity scores in multiple cohorts of patients with SLE. Lupus Sci. Med. *2*, e000080.

Lai, J.H., Lin, Y.L., and Hsieh, S.L. (2017). Pharmacological intervention for dengue virus infection. Biochem. Pharmacol. *129*, 14–25.

Lai, J.H., Wang, M.Y., Huang, C.Y., Wu, C.H., Hung, L.F., Yang, C.Y., Ke, P.Y., Luo, S.F., Liu, S.J., and Ho, L.J. (2018). Infection with the dengue RNA virus activates TLR9 signaling in human dendritic cells. EMBO Rep. *19*, e46182.

Liu, W., Chen, B., Chen, L., Yao, J., Liu, J., Kuang, M., Wang, F., Wang, Y., Elkady, G., Lu, Y., et al. (2019). Identification of fish CMPK2 as an interferon stimulated gene against SVCV infection. Fish Shellfish Immunol. *92*, 125–132.

Ngono, A.E., and Shresta, S. (2018). Immune response to dengue and Zika. Annu. Rev. Immunol. *36*, 279–308.

Paessler, S., and Walker, D.H. (2013). Pathogenesis of the viral hemorrhagic fevers. Annu. Rev. Pathol. *8*, 411–440.

Pearce, E.L., and Pearce, E.J. (2013). Metabolic pathways in immune cell activation and quiescence. Immunity *38*, 633–643.

Riley, J.S., and Tait, S.W. (2020). Mitochondrial DNA in inflammation and immunity. EMBO Rep. *21*, e49799.

Sire, J., Querat, G., Esnault, C., and Priet, S. (2008). Uracil within DNA: an actor of antiviral immunity. Retrovirology *5*, 45.

Valadao, A.L., Aguiar, R.S., and de Arruda, L.B. (2016). Interplay between inflammation and cellular stress triggered by Flaviviridae viruses. Front. Microbiol. *7*, 1233.

van der Burgh, R., and Boes, M. (2015). Mitochondria in autoinflammation: cause, mediator or bystander? Trends Endocrinol. Metab. *26*, 263–271.

Weil, A.F., Ghosh, D., Zhou, Y., Seiple, L., McMahon, M.A., Spivak, A.M., Siliciano, R.F., and Stivers, J.T. (2013). Uracil DNA glycosylase initiates degradation of HIV-1 cDNA containing misincorporated dUTP and prevents viral integration. Proc. Natl. Acad. Sci. U S A *110*, E448–E457.

Whitehorn, J., and Simmons, C.P. (2011). The pathogenesis of dengue. Vaccine *29*, 7221–7228.

Wu, D., Sanin, D.E., Everts, B., Chen, Q., Qiu, J., Buck, M.D., Patterson, A., Smith, A.M., Chang, C.H., Liu, Z., et al. (2016). Type 1 interferons induce changes in core metabolism that are critical for immune function. Immunity *44*, 1325–1336.

Wu, W.L., Ho, L.J., Chang, D.M., Chen, C.H., and Lai, J.H. (2009). Triggering of DC migration by dengue virus stimulation of COX-2-dependent signaling cascades in vitro highlights the significance of these cascades beyond inflammation. Eur. J. Immunol. *39*, 3413–3422.

Xu, Y., Johansson, M., and Karlsson, A. (2008). Human UMP-CMP kinase 2, a novel nucleoside monophosphate kinase localized in mitochondria. J. Biol. Chem. *283*, 1563–1571.

Yan, Y., Chen, R., Wang, X., Hu, K., Huang, L., Lu, M., and Hu, Q. (2019). CCL19 and CCR7 expression, signaling pathways, and adjuvant functions in viral infection and prevention. Front. Cell Dev. Biol. *7*, 212.

Zhong, Z., Liang, S., Sanchez-Lopez, E., He, F., Shalapour, S., Lin, X.J., Wong, J., Ding, S., Seki, E., Schnabl, B., et al. (2018). New mitochondrial DNA synthesis enables NLRP3 inflammasome activation. Nature *560*, 198–203.

STAR★METHODS

KEY RESOURCES TABLE

REAGENT or RESOURCE	SOURCE	IDENTIFIER
Antibodies		
CMPK2 (Western Blotting)	Abcam	Cat# Ab194567
CMPK2 (Confocal Microscopy)	GeneTex	Cat# GTX31502
CMPK2 (Western Blotting)	ATLAS	Cat# HPA041430, RRID:AB_10796674
DENV NS1	Genetex	Cat# GTX1033, RRID:AB_1240703
DENV NS2B	Genetex	Cat# GTX124246, RRID:AB_11170698
DENV NS3	Genetex	Cat# GTX629477, RRID:AB_2801283
Flag	Sigma	Cat# F1804, RRID:AB_262044
β-actin	Genetex	Cat# GTX109639, RRID:AB_1949572
Tom20	Abcam	Cat# ab186734, RRID:AB_2716623
α-tubulin	Novus	Cat# NB100-690, RRID:AB_521686
TLR-9	Abcam	Cat# ab53396, RRID:AB_883065
8-OHdG	Millipore	Cat# AB5830, RRID:AB_92060
IL-1β	Cell signaling	Cat# 12242, RRID:AB_2715503
CKR-7(4B12)FITC-(Mus musculus)	Santa Cruz	Cat# sc-57074, RRID:AB_782012
normal rat IgG-FITC	Santa Cruz	Cat# sc-2340, RRID:AB_737200
CCR7 (Homo sapiens)	BD PharMingen	Cat# 550937, RRID:AB_393968
STAT1	Santa Cruz	Cat# sc-592, RRID:AB_632434
pSTAT1	Epitomics	Cat# 2825-1, RRID:AB_2198144
NFκB p65	Santa Cruz	Cat# sc-109, RRID:AB_632039
Phospho-NF-κB p65 (Ser536)	Cell signaling	Cat# 3031, RRID:AB_330559
Purified Mouse IgM, λ Isotype Control	BD PharMingen	Cat# 550963, RRID:AB_393980
Goat IgG isotype control	Genetex	Cat# GTX35039, RRID:AB_10623176
PE Armenian Hamster IgG Isotype Ctrl	Biolegend	Cat# 400907, RRID:AB_326593
FITC Mouse IgG2a, κ Isotype Ctrl (FC)	Biolegend	Cat# 341051, RRID:AB_400209
FITC anti-mouse I-Ak (Aβk) (MHC class II)	Biolegend	Cat# 109905, RRID:AB_313454
Donkey anti-Goat IgG (H+L), Alexa Fluor 488	Thermo Fisher Scientific	Cat# A-11055, RRID:AB_2534102
Goat anti-Mouse IgG, Alexa Fluor 488	Thermo Fisher Scientific	Cat# A-11001, RRID:AB_2534069
Goat anti-Rabbit IgG (H+L), Alexa Fluor 594	Thermo Fisher Scientific	Cat# A-11012, RRID:AB_141359
Goat anti-Rabbit IgG (H+L), Alexa Fluor 647	Thermo Fisher Scientific	Cat# A27040, RRID:AB_2536101
GFP	Genetex	Cat# GTX113617, RRID:AB_1950371
PE anti-mouse CD11c	Biolegend	Cat# 117307, RRID:AB_313776
Bacterial and virus strains		
DENV2 strain New Guinea C	provided by Dr. YL Lin	N/A
DENV1	provided by Dr. YL Lin	N/A
DENV3	provided by Dr. YL Lin	N/A
DENV4	provided by Dr. YL Lin	N/A
Chemicals, peptides, and recombinant proteins		
MitoSOX	Thermo Fisher Scientific	Cat# M36008
Mitotracker deep red FM	Invitrogen	Cat# M22426

(*Continued on next page*)

Continued

REAGENT or RESOURCE	SOURCE	IDENTIFIER
Cell Counting Kit-8 (CCK-8)	Dojindo	Cat# CK04
Ponceau S	Sigma	Cat# P7170
LPS	InvivoGen	Cat# tlrl-3pelp
ATP	Sigma	Cat# A6419
Lipofectamine 3000	Thermo Fisher Scientific	Cat# L3000001
FAM-FLICA® Caspase-1 Assay Kit	Immunochemistry technologies	Cat# 97
Human GMCSF	R&D systems	215-GM
Human recombinant IL-4	R&D systems	204-IL
Mouse GMCSF	PeproTech	Cat#31503
Mouse MCSF	PeproTech	Cat#31502
Recombinant Human IFN-α	PBL Assay Science	Cat#11100-1
Recombinant mouse IFN-α	PBL Assay Science	Cat#12100-1
Recombinant Human CCL19/MIP-3β	R&D systems	Cat#361-MI-025
Recombinant Murine CCL19/MIP-3β	PeproTech	Cat#250-27B
ELISA Human IFN-α	PBL Assay Science	Cat#41100-1
ELISA Human IFN-λ1	R&D systems	Cat#DY7246
Human IL-1β Antibody (ELISA)	R&D systems	Cat# MAB601, RRID:AB_358545
Human IL-1β Biotinylated Antibody (ELISA)	R&D systems	Cat# BAF201, RRID:AB_356214
Recombinaant Human IL-1β Antibody (ELISA)	R&D systems	Cat# 201-LB
ELISA Human TNF-α	R&D system	Cat#DY210 , RRID:AB_2848160
Human CD14+ microbeads	Miltenyi Biotec	Cat#130-050-201, RRID:AB_2665482
Ruxolitinib	Invivogen	Cat#tlrl-rux
BMS-986165	MedChemExpress	Cat#HY-117287
AG490	TOCRIS	Cat#0414
STAT3 inhibitor V	Calbiochem	Cat#573099
PD985059	Calbiochem	Cat#513000
SB203580	Calbiochem	Cat#559399
SP600125	Calbiochem	Cat#420119
LY294002	Sigma-Aldrich	Cat#L9908
BAY11-7082	Calbiochem	Cat#196870
Deposited data		
Gene microarray data	This report	GEO:GSE172293
Experimental models: Cell lines		
A549	Bioresource Collection and Research Center, Taiwan	Cat# 60074, RRID:CVCL_0023
THP-1	ATCC	Cat# TIB-202, RRID:CVCL_0006
HEK293T	Gift from RNAi core, Academic Sinica, Taipei, Taiwan	N/A
Experimental models: Organisms/strains		
C57BL/6J	National Laboratory Animal Breeding and Research Center (Taipei, Taiwan)	Stock number: RMRC11005
C57BL/6J Ifnar-/-	From Dr. Guann-Yi Yu (National Health Research Institute (NHRI), Taiwan)	N/A
C57BL/6J Stat1-/-	from Dr. Chien-Kuo Lee (National Taiwan University, Taiwan)	N/A

(*Continued on next page*)

Continued

REAGENT or RESOURCE	SOURCE	IDENTIFIER
Oligonucleotides		
siRNA CMPK2 (Homo sapiens) GACCCAGUCAGUGGCAGAUUCACUU	Invitrogen	Cat#HSS151614
siRNA CMPK2 (Mus musculus) GGCAGUACUUGACCUAGUU	MDBIO, INC	N/A
sgRNA CMPK2 (Homo sapiens) GCCCTGGCTCACTTCGCCCT	Academia Sinica RNAi core	N/A
Primers for qPCR, see Table S1	This study	N/A
Recombinant DNA		
TMPK2-GFP (CMPK2-GFP)	Gift from Dr. Chang, Zee-Fen	N/A
PUC-GFP		N/A
pcDNA3.1-Mouse CMPK2-DYK	GenScript. Inc. (Piscataway, NJ)	Cat#OMu15173
pcDNA3.1-DYK		
Lenti-pLKO_AS3w.puro	Academia Sinica RNAi core	N/A
Lenti-pLKO_AS3w.puro-DYK	This study	N/A
Lenti-pLKO_AS3w.puro-mCmpk2-DYK	This study	N/A
Software and algorithms		
GraphPad Prism 7.0 software	GraphPad Software	http://www.graphpad.com/
Image J	NIH	https://imagej.nih.gov/ij/
FlowJo	FlowJo software	https://www.flowjo.com/

RESOURCE AVAILABILITY

Lead contact

Further information and requests for resources and reagents should be directed to and will be fulfilled by the lead contact, Ling-Jun Ho (lingjunho@nhri.org.tw)

Materials availability

Plasmids/stable reagents in this study are available with a completed Materials Transfer Agreement Request for these reagents by submitting to Dr. L.-J. Ho (lingjunho@nhri.edu.tw) or J.-H. Lai (laiandho@gmail.com).

Data and code availability

Sequence data that support the findings of this study are shown in the supplementary tables. The microarray datasets generated and/or analyzed in this study are available in the NCBI GEO repository (GSE172293).

EXPERIMENTAL MODEL AND SUBJECT DETAILS

Cell culture and reagents

A549 human lung epithelial cells (Bioresource Collection and Research Center, Taiwan) and HEK-293T cells (RNAi core, Academic Sinica, Taipei, Taiwan) were maintained in F12 medium and DMEM, respectively, supplemented with 10% fetal bovine serum (FBS) in a humidified atmosphere containing 5% CO_2 at 37°C. Human monocytic THP-1 cells were cultured in RPMI 1640 medium containing 10% FBS. Information about the antibodies, reagents and plasmids used in this study is given in key resources table.

DENV preparation and infection

Preparation of DENV was performed according to our report (Ho et al., 2005). The DENV2 strain New Guinea C and DENV1, DENV3 and DENV4 serotypes, which were kindly provided by Dr. YL Lin (Academic Sinica, Taipei, Taiwan), were propagated in C6/36 mosquito cells in RPMI medium containing 5% heat-inactivated FBS and maintained at 28°C for 7 days. Preparation of mock conditioned medium was performed

using the same procedures, except buffered saline was substituted for virus inoculation. Unless otherwise specified, cells were mock infected or infected with DENV at designated MOI for 2 h at 37°C. The determination of the viral titer was performed according to the methods described in our previous report (Ho et al., 2005).

Preparation of human monocyte-derived dendritic cells and mouse bone marrow-derived macrophages (BMDMs) and bone marrow-derived dendritic cells (BMDCs)

Human monocyte-derived dendritic cells were prepared with consistent quality (Lai et al., 2018). After collection of peripheral blood mononuclear cells (PBMCs), the $CD14^+$ monocytes were isolated from PBMCs using a magnetic-activated cell sorting cell isolation column (Miltenyi Biotec). The use of human blood samples was approved by the Institutional Review Board of Chang Gung Memorial Hospital (Linkou, Taiwan). The purified monocytes were cultured in RPMI 1640 medium containing 10% FBS, 800 U/ml GM-CSF and 500 U/ml IL-4 at a cell density of 1×10^6 cells/ml. The culture medium was replaced every other day with fresh medium containing GM-CSF and IL-4, and dendritic cells with a purity greater than 95% after 5–7 days of culture were used in the experiments (Ho et al., 2005). The preparation of mouse BMDMs and BMDCs was performed according to the protocol of a published report and our previous report (Bonilla et al., 2013; Lai et al., 2018). In brief, male C57BL/6 mice (6-12 weeks) were purchased from the National Laboratory Animal Breeding and Research Center (Taipei, Taiwan). The *Ifnar-/-* mice were from Dr. Guann-Yi Yu (National Health Research Institute (NHRI), Taiwan) and *Stat1-/-* mice were provided by Dr. Chien-Kuo Lee (National Taiwan University, Taiwan). All of the animal studies were conducted in accordance with a protocol approved by the Institutional Animal Care and Use Committee of the National Health Research Institute (NHRI; NHRI-IACUC-107159-A-S01). Bone marrow was flushed from the tibias and femurs of mouse hind legs using a needle syringe loaded with DMEM. After washing and filtering through a 40-μm nylon cell strainer, bone marrow cells were cultured in medium containing 20 ng/mL MCSF or GMCSF (PeproTech Inc., New Jersey, USA) for BMDM or cultured in RPMI with 10 ng/ml of mGM-CSF (PeproTech Inc., New Jersey, USA) for 6 days with the medium refreshed every 2-3 days for BMDCs.

METHOD DETAILS

Information about the antibodies, reagents and plasmids used in this study is given in key resources table.

Preparation of cytosolic and mitochondrial fraction

A Mitochondria/Cytosol Fractionation Kit from Abcam (Cambridge, UK) was used to extract mitochondrial and cytosolic fractions as described by the manufacturer. Cells (2×10^7) were resuspended in 0.3 ml of 1X Cytosol Extraction Buffer Mix containing DTT and protease inhibitors. After incubation on ice for 10 min, cells were homogenized in an ice-cold Dounce tissue grinder (150-200 passes with the grinder). The homogenate was centrifuged at 700 x g in a microcentrifuge for 10 min at 4°C and the supernatant was then centrifuged at 10,000 x g in a microcentrifuge for 30 min at 4°C. After this, the supernatant was collected (cytosolic fraction) and the pellet (intact mitochondria) was re-suspended in 50 μl of the Mitochondrial Extraction Buffer Mix containing DTT and protease inhibitors (mitochondrial fraction).

siRNA transfection

Cells were collected and resuspended at 1×10^7/ml in modified Eagle's minimum essential medium (opti-MEM, Invitrogen) containing 300 nM designated siRNA (Stealth RNAi™ siRNA, Invitrogen). Electroporation was performed using a BTX electroporator (San Diego, CA) with a profile of one pulse at 300 V for 3 ms. The cells ($2x10^6$) were then seeded in culture medium (Invitrogen, Carlsbad, CA, USA) containing 10% FBS for 24 h before subsequent treatment. For the A549 cell line, according to the manufacturer's instructions, cells were transfected with 50 nM siRNA by using Lipofectamine 3000 (Invitrogen). After transfection for 4 h, the culture medium was replaced with fresh complete medium for further experiments.

CMPK2-knockout THP-1 cells

CMPK2 sgRNA was designed and cloned into a CRISPR-Casp9 lentivector by the National RNAi Core Facility (RNA technology platform and gene manipulation core, Academia Sinica, Taiwan). The CMPK2 sgRNA lentivirus was produced after confirming the sequence and knockout efficiency. THP-1 cells were transduced with the lentivirus containing CMPK2 sgRNA in the presence of polybrene (4 μg/ml) for 48 h. Then, puromycin (5 μg/ml) was added to the culture medium for 10 days with regular replacement of the medium to eliminate untransduced cells. Subsequently, a single CRISPR-Cas9 CMPK2-knockout (KO)

THP-1 clone was selected in 96-well plates after several rounds of serial dilutions. Successful KO was confirmed by Western blotting and DNA sequencing.

Overexpression of CMPK2 in BMDCs and A549 cells

The mouse CMPK2-DYK and DYK genes were purchased from GenScript. Inc. (Piscataway, NJ) and subcloned into the PLKO_AS3w.puro. lentivector according to the manufacturer's instructions (GenScript, Piscataway, NJ, USA). The correctness of the subcloning was confirmed by sequencing. For overexpression of CMPK2 in cells, BMDCs were transduced with the lentivirus (MOI of 2), and 8 μg/ml polybrene was added on day 2 and day 5. On day 7, the cells were used for designated experiments. For overexpression of CMPK2 in A549 cells, the indicated concentrations of human CMPK2-GFP or GFP were transfected into A549 cells with Lipofectamine 3000 reagent according to the manufacturer's instructions.

Quantitative RT-qPCR

Total RNA was isolated from treated cells with NucleoZOL reagent (Macherey-Nagel, Duren, Germany) according to the manufacturer's instruction. RNA concentrations were measured using a NanoDrop spectrophotometer (ND 1000 V.3.1.0; Thermo Fisher Scientific, Waltham, MA, USA). Reverse transcription was performed with a 20-μl mixture containing 2 μg of total RNA, random hexamers (Invitrogen), and a mixture containing 10× reverse transcription buffer, dNTPs, magnesium chloride, dithiothreitol (Invitrogen), and Moloney Murine Leukemia Virus Reverse Transcriptase (MMLV RTase, Invitrogen). cDNA was prepared for further evaluation using qPCR. Briefly, 20 ng of cDNA was amplified in a total mixture volume of 20 μl consisting of 1× KAPA SYBR FAST qPCR Master Mix (KAPA Biosystems, Boston, MA, USA) and the appropriate gene-specific primers, which were added at a final concentration of 200 nM. The primers used are shown in Table S1. The reaction conditions were 40 cycles comprising steps at 95°C for denaturing and 60°C for annealing and extension on a LightCycler 480 (Roche). The changes in gene expression induced by DENV infection in the presence or absence of inhibitors or siRNA were calculated with the following formula: fold change = $2^{-\Delta\,(\Delta Ct)}$, where ΔCt = Ct of target gene − Ct of GAPDH, and Δ(ΔCt) = ΔCt infected − ΔCt mock control.

Extraction of total and cytosolic DNA and mtDNA measurement

Total and cytosolic DNA extraction method was performed (Lai et al., 2018) with some modification. Cells (4×10^6) were divided into two equal aliquots. One aliquot, for normalization control, was used to extract total DNA using a NucleoSpin Tissue kit (Macherey-Nagel, Duren, Germany). The other was resuspended in 400 μl of buffer containing 150 mM NaCl, 50 mM HEPES pH 7.4, and 25 mg/ml digitonin (EMD Chemicals, Gibbstown, NJ, USA). After rotaion end-over-end for 15–20 min at 4°C, the samples were then centrifuged at 980 × g for 3 min three times to remove cellular debris. The supernatants were collected and spun at 17,000 × g for 10 min to remove the remaining cellular residue and to yield cytosolic preparations free of nuclear, mitochondrial, and endoplasmic reticulum contamination. The DNA in the cytosol fraction was then isolated by running the sample through a NucleoSpin Tissue column (Macherey-Nagel) and subsequently eluted with buffer.

To measure the levels of mtDNA, 20 ng of isolated DNA was subjected to qPCR with KAPA SYBR FAST qPCR Master Mix (KAPA Biosystems) with 200 nM mtDNA primers (16S and ND5 for THP1 cells; 12S and D-loop for BMDCs) or nuclear DNA (nDNA) primers (B2M and TERT for THP-1 cells; actin and albumin for BMDCs). Two mtDNA primer pairs were used to quantify mtDNA. The levels of mtDNA in total cell lysates were calculated as mtDNA normalized to nDNA. To quantify mtDNA in the cytosolic fraction, 20 ng of a purified plasmid encoding the FLAG gene (PCR3.1-flag) was added to the eluted solution according to the protocol published by Aguirre et al. (Aguirre et al., 2017), except that the FLAG gene was used instead of the enhanced green fluorescent protein (EGFP) gene. The specific primers for both endogenous mtDNA and the FLAG plasmid were used to measure the relative content of cytosolic mtDNA expression normalized to that of FLAG (the primers for PCR are given in Table S1). The relative mtDNA abundance indicates the relative mtDNA content in DENV-infected cells normalized to that in mock-infected cells.

Western blotting

Enhanced chemiluminescence Western blotting (Amersham, GE Healthcare Life Science, Uppsala, Sweden) was performed to study protein levels (Hsu et al., 2016). Briefly, proteins were separated on a 10% SDS-PAGE gel and transferred to a nitrocellulose membrane. For immunoblotting, the nitrocellulose

membrane was incubated with TBS-T containing 5% nonfat milk for 1 h and then blotted with an Ab against a specific protein overnight. After washing with TBS-T, the membrane was incubated with secondary antibodies conjugated to horseradish peroxidase for 1 h. The membrane was then incubated with a substrate and exposed to X-ray film. After scanning, the intensities of the bands on the Western blot were compared using ImageJ software.

Flow cytometry

The method used to assess the expression of cell-surface marker CCR7, intracellular 8-OHdG, TLR-9, and active-caspase-1 has been described (Lai et al., 2018; Wu et al., 2009). In brief, treated cells were collected, washed twice with cold PBS and then stained with fluorophore-conjugated antibodies specific for designated molecules at 4°C for 1 h. The cells were then analyzed and quantified using flow cytometry. Data were processed and analyzed with CellQuest software (BD Biosciences).

Measurement of mitochondrial ROS levels

For mtROS level measurement, cells were incubated with 5 μM MitoSOX™ Red (Invitrogen) in culture medium for 30 min at 37°C. After washing with PBS, the cells were analyzed with flow cytometry (Lai et al., 2018).

Determination of cytokine concentrations via ELISA

Standard ELISA were used to measure the concentrations of cytokines such as IFN-λ and TNF-α (R&D Systems), IFN-α (PBL Assay Science, Piscataway, NJ, USA) and IL-1β (R&D Systems).

CCK-8 cell viability assay

Cell Counting Kit-8 (CCK-8) (Dojindo Laboratories, Kumamoto, Japan) was used to measure cell viability according to the protocol (Lai et al., 2018). Cells were seeded in 96-well plates overnight. CCK-8 reagents were then added and incubated for 2 h at 37°C. The OD values for each well were read at a wavelength of 450 nm on a microplate reader. The viability of cells (%) was determined by subtracting the OD of experimental wells from the OD of the blank well and dividing by the OD of the control group well.

Immunofluorescence staining and confocal imaging

Cells were collected and washed two times with PBS before being fixed with 4% paraformaldehyde on ice for 20 min. The fixed cells were washed and resuspended homogenously in PBS with 0.05% Triton X-100 on ice for 5 min to permeabilize the cells. The cells were washed again with PBS and blocked with PBS containing 1% mouse FcR Blocking Reagent (Miltenyi Biotech, Bergisch Gladbach, Germany) for 30 min. Primary antibodies were added and incubated with the cells for 2 h at room temperature. After removing unbound antibodies by washing, secondary antibodies conjugated with an Alexa Fluor fluorescent dye were added and incubated in the dark for 1 h at room temperature. Cell nuclei were counterstained with 1 mg/ml DAPI (4′, 6-diamidino-2-phenylindole; Sigma) at a 1:5000 dilution. Finally, 2×10^3 cells were seeded on slides, air dried in the dark and mounted with mounting reagent (FluorSave™ Reagent, EMD Millipore Calbiochem, San Diego, CA, USA) for subsequent confocal microscopy analysis. Samples were examined with a Leica TCS SP5 confocal laser scanning microscope (Leica Microsystems, Wetzlar, Germany) equipped with an HCX PL APO 63×/1.4-0.6 oil objective (Leica). Image processing and colocalization analysis were performed with Leica LAS AF software as described in our previous report (Lai et al., 2018).

Caspase 1 activity assay

The activity of caspase-1 was evaluated according to the instructions provided with the FAM FLICA Caspase 1 Assay Kit (Molecular Probes). After treatment, cells were collected and washed with PBS twice. Subsequently, the cell pellet was resuspended in 100 μl of medium and incubated with a 30x FLICA solution (3.3 μl/sample) for 60 min at 37°C in the dark. After washing with washing buffer (provided with the kit), the cells were subsequently resuspended in 1 ml of wash buffer for further flow cytometry (Attune NxT) and FlowJo analysis.

Chemotaxis assay

Chemotaxis assays were performed to study cell migration (Hsu et al., 2016). Cells migrating through a polycarbonate filter (pore size of 5 μm for BMDCs and 8 μm for THP-1 cells) in 24-well Transwell chambers (Corning Costar, Corning Incorporated Life Sciences, Tewksbury, MA, USA) were evaluated. The lower

chamber of the Transwell system contained serum-free RPMI medium containing 600 µl of 0.1% BSA with or without 100 ng/ml CCL19 (R&D Systems). Cells (1×10^5) in 100 µl of serum-free medium containing 0.1% BSA were loaded in the upper chamber and incubated for 16 h at 37 °C. Then, the cells migrating from the upper chamber to the lower chamber were counted by flow cytometry. CellQuest software was used to evaluate the acquired events during a fixed time period of 60 s on a FACScan.

QUANTIFICATION AND STATISTICAL ANALYSIS

All variables representing pooled donors are expressed as the mean ± SEM. Statistical comparisons were performed using Student's T-test or one-way analysis of variance (ANOVA). When ANOVA showed significant differences among groups, Bonferroni's post hoc test was used to identify the specific pairs of groups that significantly differed. A p value < 0.05 was considered statistically significant. Asterisks indicate values that are significantly different from the relevant control (*$p < 0.05$, **$p < 0.01$, ***$p < 0.001$ and ****$p < 0.0001$).